

# Physiological and molecular responses of different rose (*Rosa hybrida* L.) cultivars to elevated ozone levels

Hua Wang<sup>1,2,3</sup> | Maofu Li<sup>1,2,3</sup>  | Yuan Yang<sup>1,2,4</sup> | Pei Sun<sup>1,2,3</sup> |  
 Shuting Zhou<sup>1,2,3</sup> | Yanhui Kang<sup>1,2,3</sup> | Yansen Xu<sup>5</sup> | Xiangyang Yuan<sup>5</sup> |  
 Zhaozhong Feng<sup>5</sup> | Wanmei Jin<sup>1,2,3</sup> 

<sup>1</sup>Institute of Forestry and Pomology, Beijing Academy of Agriculture and Forestry Sciences, Beijing, China

<sup>2</sup>Key Laboratory of Biology and Genetic Improvement of Horticultural Crops (North China), Ministry of Agriculture and Rural Affairs, Beijing, China

<sup>3</sup>Beijing Engineering Research Center of Functional Floriculture, Beijing, China

<sup>4</sup>Beijing Engineering Research Center for Deciduous Fruit Trees, Beijing, China

<sup>5</sup>School of Applied Meteorology, Nanjing University of Information Science & Technology, Nanjing, China

## Correspondence

Zhaozhong Feng, School of Applied Meteorology, Nanjing University of Information Science & Technology, Nanjing 210044, China.

Email: [zhaozhong.feng@nuist.edu.cn](mailto:zhaozhong.feng@nuist.edu.cn)

Wanmei Jin, Institute of Forestry and Pomology, Beijing Academy of Agriculture and Forestry Sciences, Beijing 100093, China.

Email: [jwm0809@163.com](mailto:jwm0809@163.com)

## Funding information

National Natural Science Foundation for Young Scholars of China, Grant/Award Number: 31600418; Science and Technology Innovation Ability Construction Projects of Beijing Academy of Agriculture and Forestry Science, Grant/Award Numbers: KJCX20230110, KJCX20210415

## Abstract

The increasing ground-level ozone (O<sub>3</sub>) pollution resulting from rapid global urbanization and industrialization has negative effects on many plants. Nonetheless, many gaps remain in our knowledge of how ornamental plants respond to O<sub>3</sub>. Rose (*Rosa hybrida* L.) is a commercially important ornamental plant worldwide. In this study, we exposed four rose cultivars (“Schloss Mannheim,” “Iceberg,” “Lüye,” and “Spectra”) to either unfiltered ambient air (NF), unfiltered ambient air plus 40 ppb O<sub>3</sub> (NF40), or unfiltered ambient air plus 80 ppb O<sub>3</sub> (NF80). Only the cultivar “Schloss Mannheim” showed significant O<sub>3</sub>-related effects, including foliar injury, reduced chlorophyll content, reduced net photosynthetic rate, reduced stomatal conductance, and reduced stomatal apertures. In “Schloss Mannheim,” several transcription factor genes—*HSF*, *WRKY*, and *MYB* genes—were upregulated by O<sub>3</sub> exposure, and their expression was correlated with that of *NCED1*, *PP2Cs*, *PYR/PYL*, and *UGTs*, which are related to ABA biosynthesis and signaling. These results suggest that HSF, WRKY, and MYB transcription factors and ABA are important components of the plant response to O<sub>3</sub> stress, suggesting a possible strategy for cultivating O<sub>3</sub>-tolerant rose varieties.

## KEYWORDS

molecular response, ozone, physiological responses, rose, sensitivity

## 1 | INTRODUCTION

Ozone (O<sub>3</sub>) is a secondary pollutant formed by the photochemical reaction between the precursor pollutants nitrogen oxide (NOx) and

volatile organic compounds (VOCs) (Wang et al., 2022). Due to rapid urbanization and industrialization, tropospheric O<sub>3</sub> concentrations have more than doubled since the start of the Industrial Revolution, which has adverse effects on trees, crops, and natural vegetation

This is an open access article under the terms of the [Creative Commons Attribution-NonCommercial-NoDerivs](https://creativecommons.org/licenses/by-nc-nd/4.0/) License, which permits use and distribution in any medium, provided the original work is properly cited, the use is non-commercial and no modifications or adaptations are made.

© 2023 The Authors. *Plant Direct* published by American Society of Plant Biologists and the Society for Experimental Biology and John Wiley & Sons Ltd.

(Chappelka & Samuelson, 1998; Feng et al., 2019, 2022; Yendrek et al., 2015). O<sub>3</sub> can induce a range of pathologies in plants, including visible leaf injury and the disruption of physiology, growth, biomass, and reproductive development (Cotrozzi, 2021; Holder & Hayes, 2022; Leisner & Ainsworth, 2012; Li et al., 2015). O<sub>3</sub> exposure has well-documented economic and environmental effects on plant productivity, but the severity of responses to O<sub>3</sub> varies by plant species and variety (Shang et al., 2020; Wang et al., 2021; Yang et al., 2016; Zhang & Sonnewald, 2017).

O<sub>3</sub> can affect the physiological and biochemical characteristics of plants, causing visible foliar injury, decreased photosynthesis, stomatal closure, chlorophyll degradation, high levels of reactive oxygen species (ROS) production, metabolic disorder, accelerated senescence, and suppressed productivity (Ainsworth, 2017; Feng et al., 2008; Han et al., 2021; Rathore & Chaudhary, 2019). Visible leaf injury induced by chronic O<sub>3</sub> exposure varies depending on the species and exposure conditions (Feng et al., 2014; Li et al., 2015; Shang et al., 2020). Several studies have revealed that the net photosynthesis rates in trees, wheat (*Triticum aestivum*), castor (*Ricinus communis* L.), and *Arabidopsis* (*Arabidopsis thaliana*) considerably decrease in response to high ambient O<sub>3</sub> concentrations, which has generally been attributed to decreased carboxylation efficiency, electron transfer between photosystems I and II, and effects on stomata (Cotrozzi, 2021; Engela et al., 2021; Feng et al., 2008; Paoletti, 2006; Rathore & Chaudhary, 2019). Stomatal conductance is a key metric of plant sensitivity to O<sub>3</sub> (Hasan et al., 2021). Several reports indicate that O<sub>3</sub> decreases stomatal conductance, consequently limiting O<sub>3</sub> uptake by leaves (Li et al., 2015; Rathore & Chaudhary, 2019). However, other reports indicate that stomata are unable to close rapidly when impaired by high O<sub>3</sub> levels (Morales et al., 2021). Notably, these studies were mainly based on tree, crops, and grass species, whereas little research has been done on the effects of ornamental plants.

Urban green spaces improve air quality, regulate climate, improve esthetics, and promote health in cities (Nowak & Dwyer, 2007) and are thus important for successful urbanization. However, these benefits may be undercut by increasing O<sub>3</sub> concentrations (Yang et al., 2016). Efforts to limit O<sub>3</sub> damage in urban plants are complicated by the fact that not only different species but even different cultivars and accessions of the same species can differ in their O<sub>3</sub> sensitivity (Rathore & Chaudhary, 2019; Shang et al., 2020; Yang et al., 2016; Zouzoulas et al., 2009). This variability can provide an opportunity to select O<sub>3</sub>-resistant varieties when planning urban green spaces likely to be exposed to O<sub>3</sub>-induced damage.

Transcriptional regulation is an early and crucial part of a plant's response to abiotic and biotic stress. Molecular responses to O<sub>3</sub> stress have been studied in several species: *Arabidopsis* (Morales et al., 2021), tomato ("Little Tom") (*Solanum lycopersicum*) (Xu et al., 2021), rice (*Oryza sativa* L.) (Ashrafuzzaman et al., 2018), soybean (*Glycine max* L. Merr.) (Leisner et al., 2014), poplar (*Populus deltoides* clone "546") (Zhang et al., 2019), silver birch (*Betula pendula* Roth) (Kontunen-Soppela et al., 2010), crabapple (*Malus* "Hongjiu") (Zhang et al., 2022), Medicago (*Medicago truncatula*) (Iyer et al., 2013), and sage (*Salvia officinalis* L.) (Marchica et al., 2019). These studies

have shown that many stress-associated genes are upregulated under elevated O<sub>3</sub>, including genes encoding transcription factors (TFs) and stress pathway components associated with signaling mechanisms, early cell death, and leaf senescence (Kontunen-Soppela et al., 2010; Leisner et al., 2014; Marchica et al., 2019; Zhang et al., 2019). O<sub>3</sub> plays an active role in promoting TF gene expression. The TFs then promote the transcription of key genes, inducing physiological and biochemical changes that lead to phenotypic variation. Thus, identifying the genes targeted by these TFs and deciphering the downstream biochemical pathways could facilitate the development of strategies to limit O<sub>3</sub> damage.

Rose (*Rosa hybrida* L.) is one of the most important ornamental plants worldwide, with great symbolic, cultural, and economic value (Cheng et al., 2021; Magnard et al., 2015; Raymond et al., 2018; Smulders et al., 2019). The genus *Rosa* contains about 200 species and over 30,000 modern rose cultivars (Leus et al., 2018). Roses have been cultivated since antiquity for their flowers and essential oils (Eugster & Märki-Fischer, 1991), are frequently used in urban greening, and are the most popular garden plants worldwide (Wang et al., 2017). Horticultural roses are increasingly used in temperate and subtropical regions as essential components of urban green spaces, with an estimated annual production of 220 million roses for landscape use (Nadpal et al., 2016; Wu et al., 2019). For example, more than 50 million roses have been planted across Beijing, China, over an area of 25,000 acres (Beijing Gardening and Greening Bureau, 2017). However, neither the molecular responses of roses to O<sub>3</sub> stress nor the sensitivity of different cultivars to O<sub>3</sub> have been well characterized.

In this study, we selected four common rose cultivars ("Schloss Mannheim," "Iceberg," "Lüye," and "Spectra") and investigated their phenotypic and molecular changes in response to elevated O<sub>3</sub>. We profiled each variety at the physiological, ultrastructural, and molecular levels. This allowed us both to investigate the complexity of the O<sub>3</sub> stress response in roses and to discover new genes and pathways likely to be modulated as part of the O<sub>3</sub> response.

## 2 | MATERIALS AND METHODS

### 2.1 | Plant material and experimental site

The experimental site was located in the Yanqing District of Beijing, China. The climate at the site is temperate and monsoonal, with four distinct seasons. Meteorological conditions including the annual mean precipitation and air temperature at this site are described in our previous paper (Xu et al., 2019).

Three-year-old plants of four rose cultivars (*R. hybrida* cv. "Schloss Mannheim," "Iceberg," "Lüye," and "Spectra") were obtained from a nearby nursery and cultivated at the Institute of Forestry and Pomology, Beijing Academy of Agriculture and Forestry Sciences, since the spring. Rose is the city flower of Beijing. We have described the distribution and features of rose plantings by surveying 546 sites covering different types of urban green spaces in the built-up areas of Beijing (Wang et al., 2017). The four rose cultivars are



widespread in the area where the study took place. “Schloss Mannheim” and “Iceberg” are floribunda rose cultivars, while “Lüye” and “Spectra” are climbing rose cultivars. “Schloss Mannheim” is orange blend and blooms in flushes throughout the season. “Iceberg” is among the top 10 roses of the world and the best landscape white around. “Lüye” is suitable for the garden roses with the vigorous growth, recurrently flowering. “Spectra” is large-flowered climber forming esthetic flower landscape. After pruning uniformly, the saplings were moved to the field station, when they were transplanted into 25-cm-diameter circular plastic pots (5 L) filled with mixed soil (local soil:nutrition soil:peat = 1:1:1). Subsequently, 180 uniform plants were placed in nine Open Top Chambers (OTCs; height and area were 3.0 m and 12.5 m<sup>2</sup>, made by toughened glass) to acclimate to the OTC environment.

## 2.2 | O<sub>3</sub> treatments

O<sub>3</sub> fumigation lasted 10 h per day (08:00–18:00), except for rainy days. Three O<sub>3</sub> treatments were applied: unfiltered ambient air (NF), unfiltered air with the targeted addition of 40 ppb O<sub>3</sub> (NF40), and unfiltered air with the targeted addition of 80 ppb O<sub>3</sub> (NF80). For each O<sub>3</sub> treatment, three OTC replicates were used (5 plants × 4 cultivars × 3 replicate OTCs × 3 O<sub>3</sub> treatments).

The O<sub>3</sub> delivery system and size of the OTCs condition have been described in our previous papers (Peng et al., 2020; Xu et al., 2019). Ozone was generated from pure oxygen using an O<sub>3</sub> generator (HY003, Chuangcheng Co., Jinan, China), mixed with ambient air by a fan (1.1 KW, 1,080 Pa, 19 m<sup>3</sup> min<sup>-1</sup>, CZR, Fengda, China), and then released into the OTCs. O<sub>3</sub> concentrations in the nine chambers were monitored using a UV absorption O<sub>3</sub> analyzer (Model 49i, Thermo Scientific, United States), and all data were stored using a data logger (CR1000, Campbell Scientific Inc., Logan, UT, United States). During the experimental period, the average daily O<sub>3</sub> concentration in the daylight at 10 h was 52.0 ± .7, 76.0 ± 1.2, and 103.6 ± .5 ppb under NF, NF40, and NF80 conditions, respectively. The level of O<sub>3</sub> accumulation over a threshold hourly O<sub>3</sub> concentration of 40 ppb in daylight hours (AOT40) was 17.1 ± .5, 37.5 ± 1.0, and 64.5 ± .3 ppm h under NF, NF40, and NF80 conditions, respectively.

## 2.3 | Physiological and biochemical analysis

Leaf samples were collected at 30, 60, 90, and 120 days after fumigation (DAF) for physiological and biochemical analysis.

## 2.4 | Visible injuries

All plants were evaluated weekly until O<sub>3</sub> symptoms first appeared and then monthly thereafter. The dates when visible injury first appeared were recorded. Plants subjected to NF and NF40/NF80 treatments were compared to confirm that elevated O<sub>3</sub> was the cause of the visible injury.

## 2.5 | Gas-exchange parameters

Two fully expanded upper Sun-leaves per plant from three different marked plants per chamber were selected to measure gas exchange at four time points: at the beginning of July, August, September, and October. Gas exchange and chlorophyll fluorescence were measured using a portable Li-Cor6400 photosynthesis system with a leaf chamber fluorometer (Li-Cor Inc., Lincoln NE, United States) from 9:00 to 11:30 at 30, 60, 90, and 120 DAF. During the measurements, CO<sub>2</sub> levels were set at 380 ppm, photosynthetic active radiation (PAR) at 1,200 mol m<sup>-2</sup> s<sup>-1</sup>, relative humidity at 50 ± 5%, and block temperature at 30 ± 2°C. Measurements of diurnal variation of gas exchange were conducted using a portable Li-Cor6400 photosynthesis system from 7:00–19:00.

## 2.6 | Photosynthetic pigments

SPAD chlorophyll meter readings (SCMR) for chlorophyll contents were made every 3 h from 7:00 to 19:00 at 30, 60, 90, and 120 DAF. The fully expanded and intact leaves from the top of the main stem were sampled for each plant.

Two leaf disks (7-mm diameter) per plant per chamber were collected and incubated in 4 ml 95% ethanol in the dark for 48 h at room temperature. The absorbance of leaf pigment extracts was measured at 664, 648, and 470 nm using a spectrophotometer (UV 4807) for chlorophyll a (Chla), chlorophyll b (Chlb), and carotene (Car), respectively. Chlorophyll contents were calculated according to the specific absorption coefficients (Lichtenthaler, 1987). All analyses were performed with three biological replicates.

## 2.7 | Measuring leaf ultrastructure

Three leaf disks (7-mm diameter) per plant per chamber were collected at 120 DAF for histological observations. The leaf disks were fixed in formaldehyde-acetic acid fixative solution (50% ethanol:glacial acetic acid:formaldehyde = 18:1:1) at 4°C no less than 24 h. Then, the leaf disks were dehydrated followed by 20 min treatments each with 70%, 80%, 90%, 95%, and 100% ethanol. After that, the plant materials were dried by CO<sub>2</sub> critical-point drying apparatus. The surface anatomy and epicuticular wax structure of leaves were observed and photographed with a scanning electron microscope (SEM, Hitachi S-4800, Tokyo, Japan) as described by Kakani et al. (2003). All images were acquired digitally using Quartz PCI software (Vancouver, BC, Canada), which was used for the image analysis.

## 2.8 | RNA-seq analysis

The molecular responses of plants to ozone exposure differed in herbs (Whaley et al., 2015) or woody plants (Zhang et al., 2019), in chronic stress (Zhang et al., 2019) or acute stress (Marchica et al., 2019).

Hereby, the choice of taking the samples at different time scales such as hours and days depends on the actual conditions. In our study, to reveal the molecular responses of rose, a woody perennial plant, to chronic ozone stress, the choice of taking the samples at 60 DAF and 120 DAF is consistent with the first and the most significant differences in physiological traits, respectively. Total RNA and the first-strand cDNA were isolated and amplified from leaves; samples were collected at 60 and 120 DAF. The sequencing of cDNA was carried by Novogene Bioinformatics Technology Co., Ltd. (Beijing, China) using Illumina HiSeq™ 2000 platform (Illumina incorporation, San Diego, California). All RNA-seq analyses were performed using three biological replicates. Use feature Counts v1.6.2 to calculate the gene alignment and FPKM. DESeq2 v1.22.1 was used to analyze the differential expression between the two groups, and the *P* value was corrected using the Benjamini and Hochberg method. The enrichment analysis is performed based on the hypergeometric test. For KEGG, the hypergeometric distribution test is performed with the unit of pathway; for GO, it is performed based on the GO term.

## 2.9 | Weighted Gene Co-Expression Network Analysis

We used Weighted Gene Co-Expression Network Analysis (WGCNA) analysis of transcriptome datasets from O<sub>3</sub> stress and control conditions in order to reveal novel genes and the molecular pathways underlying rose response to O<sub>3</sub> stress. Gene co-expression networks were constructed using the WGCNA v1.69 package in the R software. Module-trait associations were estimated using the correlation between the module eigengene and O<sub>3</sub> stress/control treatments. Network visualization for each module was performed using the Cytoscape software version 3.6.1 with a cut-off the weight parameter obtained from the WGCNA set at .3. The gene co-expression network is a scale-free weighted gene network with multiple nodes connected to different nodes via edges. Each node represents a gene, which is connected to a different number of genes. The gene that is connected to a greater number of genes is denoted with a bigger size and is more important for its interaction with other genes.

## 2.10 | qRT-PCR validation

Leaf samples were collected at 30, 60, 90, and 120 DAF for molecular analysis, which is consistent with gas-exchange measurements. The expression level of key genes in red and yellow modules, MYB TFs involved in abiotic stress (*RhMYB62* and *RhMYB108*) (Wu et al., 2022), and genes involved in ABA signaling pathway (*NCED1*, *OST1*, and *BG1*) (Carvalho et al., 2016) were also detected and verified by qRT-PCR as described previously (Jin et al., 2016). Primers were designed using Primer 5.0 (Premier Biosoft International, Palo Alto, CA), as shown in Tables S1 and S2 and acquired from Sangon Inc. (Sangon, Shanghai, China). Total RNA and first-strand cDNA were isolated and amplified from rose leaves. qRT-PCR was conducted

with a Bio-Rad CFX96 Real-Time PCR Detection System (Bio-Rad, CA) using a 10- $\mu$ l reaction mixture comprising 5  $\mu$ l SYBR Premix (Bio-Rad, CA), 1  $\mu$ l forward primer (10  $\mu$ M), 1  $\mu$ l reverse primer (10  $\mu$ M), 1  $\mu$ l cDNA template (20 ng), and 2  $\mu$ l ddH<sub>2</sub>O. The amplification program consisted of one cycle of 95°C for 5 min, followed by 40 cycles of 95°C for 5 s and 60°C for 15 s. The melting curves were obtained using the following cycling parameters: 65°C for 5 s, followed by heating at .5°C increments to a final temperature of 95°C, with continuous fluorescence collection. Finally, the transcript levels of different genes were analyzed using the  $2^{-\Delta\Delta CT}$  method (Livak & Schmittgen, 2001). The expression levels of  $\beta$ -actin were used as an internal control. All analyses were performed with three biological replicates.

## 2.11 | Statistical analyses

Differences and interactive effects between the O<sub>3</sub> treatments and cultivars/different time points among parameters (gas-exchange parameters, photosynthetic pigments, and gene expression) were measured by three-way ANOVA, with O<sub>3</sub> treatments, cultivars, and different time points as independent factors. Post hoc comparisons were completed using the Tukey's HSD test. Prior to analysis, data were checked for normality (Kolmogorov-Smirnov test) and homogeneity of variance (Levene's test). Otherwise, one-way ANOVA (analysis of variance) with post hoc test was used to compare whether there were statistically significant differences among all treatments within each sampling time. A difference between the means was considered significant if *p* < .05. All the data in the figures are shown as mean  $\pm$  standard error. All the analyses were performed with SPSS statistics software (Version 16.0, SPSS Inc., Chicago, IL, United States).

## 3 | RESULTS

### 3.1 | O<sub>3</sub> causes detectable leaf damage

Injury responses to O<sub>3</sub> varied significantly by cultivar. In *R. hybrida* cv. "Schloss Mannheim," white chlorotic spots first appeared on older leaves in the NF40 treatment group, when AOT40 was 9.0 ppm h or on older leaves exposed to NF80 treatment, when AOT40 was also 9.0 ppm h, although symptoms were more severe for NF80. With prolonged exposure to O<sub>3</sub>, white chlorotic spots expanded to all upper leaf surfaces and spread into yellowing chlorotic patches, leading to brown stains on the upper leaf surfaces by 60, 90, and 120 DAF in both the NF40 and NF80 treatments. Both prolonged exposure time and increased exposure concentration accelerated the symptoms of foliar injury in "Schloss Mannheim" (Figure 1). By contrast, no symptoms were observed for *R. hybrida* cv. "Iceberg," "Lüye," and "Spectra" hybrids (Figure 1). There are many potential phenotypic responses to O<sub>3</sub>, but from the perspective of visible foliar injury, the "Schloss Mannheim" cultivar was clearly the most sensitive to O<sub>3</sub>.

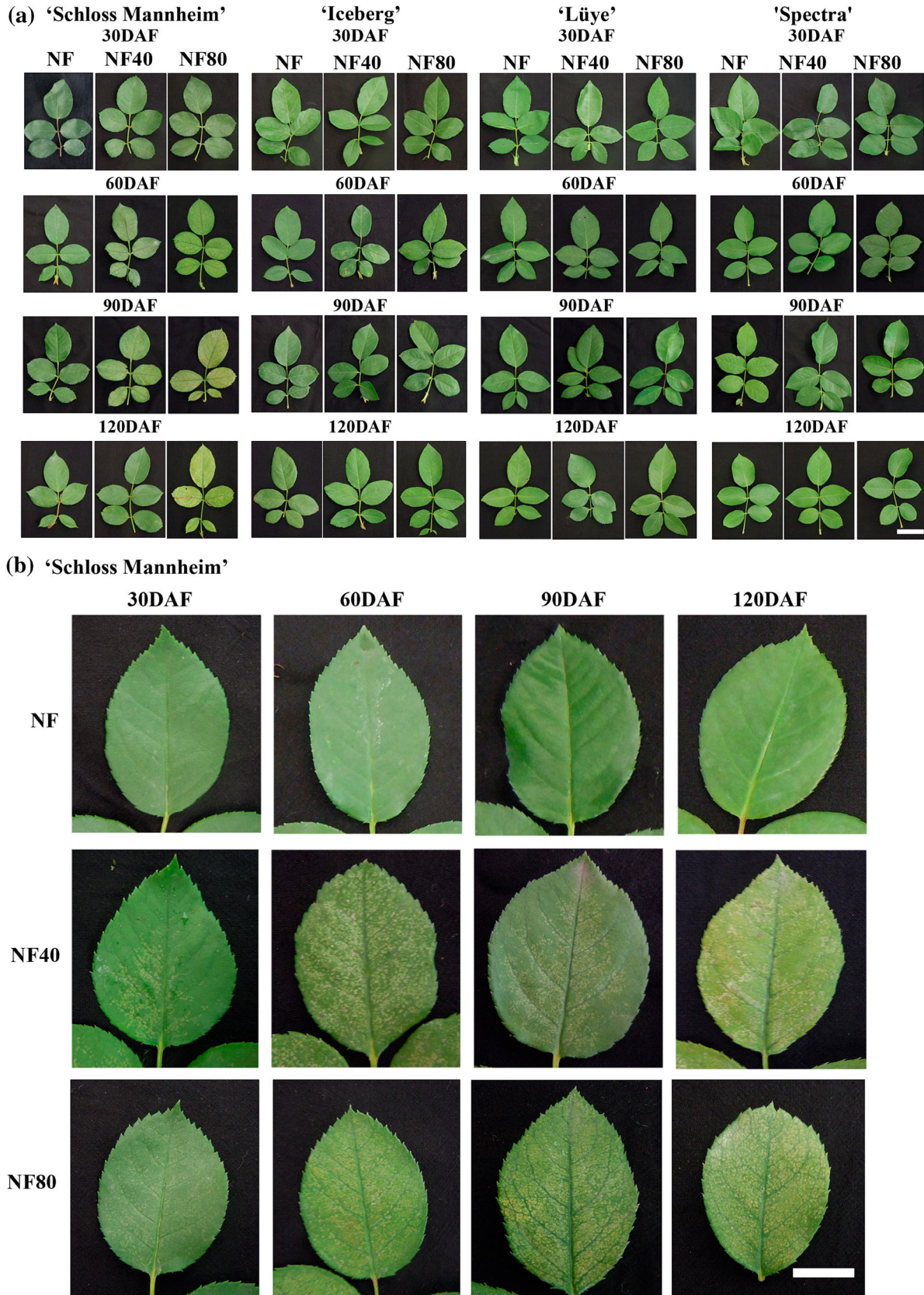


**FIGURE 1**  $O_3$  foliar injury symptoms were detected in the leaves of “Schloss Mannheim” but not the other rose cultivars under three  $O_3$  treatments at 30, 60, 90, and 120 DAF. (a)  $O_3$  foliar symptoms of “Schloss Mannheim,” “Iceberg,” “Lüye,” and “Spectra.” (b) The chlorotic spots on the leaves of the sensitive cv. “Schloss Mannheim.” NF, control treated with unfiltered ambient air; NF40, elevated  $O_3$  with the targeted addition of 40 ppb  $O_3$ ; NF80, elevated  $O_3$  with the targeted addition of 80 ppb  $O_3$ . Note: bar, 2 cm in images of compound leaves (a) and 1 cm in images of lobules (b).

### 3.2 | O<sub>3</sub> causes various physiological changes only in the O<sub>3</sub>-sensitive cultivar

Consistent with the yellowing chlorotic patches observed in “Schloss Mannheim,” treatment with increasing O<sub>3</sub> concentrations reduced chlorophyll content in the leaves of this cultivar. The chlorophyll a (Chla), chlorophyll b (Chlb), and carotenoid (Car) contents of leaves subjected to the NF40 and NF80 treatments were significantly lower than those of the control (Figure 2a). Under NF40 treatment, Chla levels decreased from 1.87 to 1.58 mg g<sup>-1</sup> at 30 DAF (15%) and from 1.40 to 1.34 mg g<sup>-1</sup> at 60 DAF (5%); these differences were not significant. However, Chla levels significantly decreased from 1.61 to 1.31 mg g<sup>-1</sup> at 90 DAF (18%) and from 1.10 to .64 mg g<sup>-1</sup> at 120 DAF (42%) (Figure 2a). Under NF80 treatment, Chla levels significantly decreased from 1.87 to 1.32 mg g<sup>-1</sup> at 30 DAF (29%), 1.40 to

1.05 mg g<sup>-1</sup> at 60 DAF (25%), 1.61 to .67 mg g<sup>-1</sup> at 90 DAF (58%), and 1.10 to .65 mg g<sup>-1</sup> at 120 DAF (41%) (Figure 2a). Thus, greater decreases in chlorophyll content were detected under NF80 versus NF40 treatment. Chlb and Car displayed a similar pattern to Chla (Figure 2b,c). By contrast, no significant reductions in chlorophyll or carotenoid contents were detected for the cultivar “Iceberg,” “Lüye,” or “Spectra.” “Schloss Mannheim” also showed large diurnal changes in chlorophyll contents between plants subjected to NF, NF40, and NF80 treatments (Figure S1).

We detected significant reductions in gas-exchange parameters for “Schloss Mannheim” under both O<sub>3</sub> treatments starting at 60 DAF (Figure 2d,e; Table S3). These parameters tended to decline with O<sub>3</sub> treatment for “Iceberg,” “Lüye,” and “Spectra,” although the differences were not significant (Figure 2d,e; Table S3). In “Schloss Mannheim,” the net photosynthesis rate (Asat) decreased by 21%,

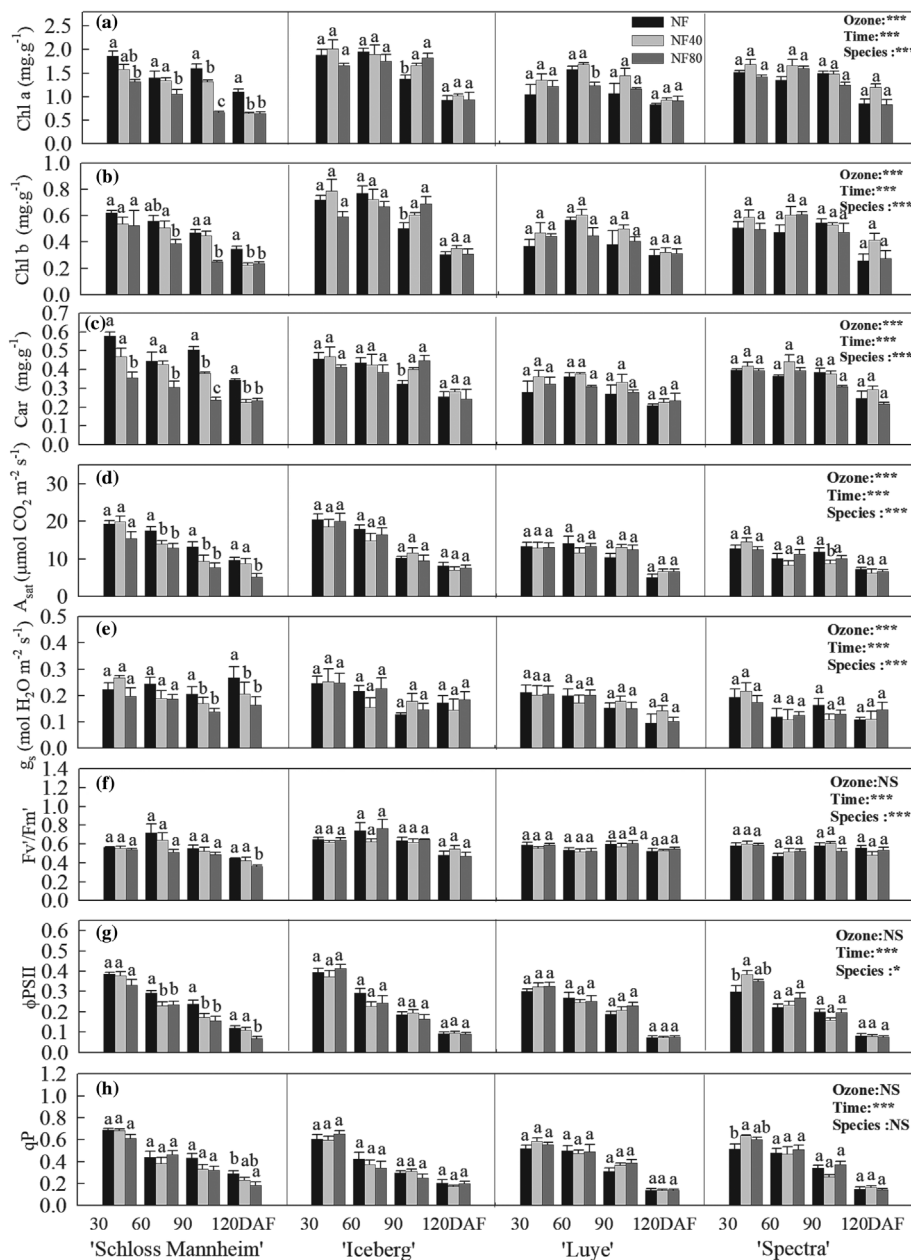


**FIGURE 2** Effects of O<sub>3</sub> on chloroplast pigment contents, gas-exchange and chlorophyll fluorescence parameters in rose cultivars “Schloss Mannheim,” “Iceberg,” “Lüye,” and “Spectra” under three treatments at 30, 60, 90, and 120 DAF. (a) Mean value (mean ± SE) of chlorophyll a (mg g<sup>-1</sup> fresh leaf) contents. (b) Mean value (mean ± SE) of chlorophyll b (mg g<sup>-1</sup> fresh leaf) contents. (c) Mean value (mean ± SE) of carotenoid (mg g<sup>-1</sup> fresh leaf) contents. (d) Mean value (mean ± SE) of net photosynthesis rates (Asat). (e) Mean value (mean ± SE) of stomatal conductance (gs). (f) Mean value (mean ± SE) of efficiency of excitation energy capture by open PSII reaction centers (F<sub>v</sub>'/F<sub>m</sub>'). (g) Mean value (mean ± SE) of quantum yield of PSII electron transport (ΦPSII). (h) Mean value (mean ± SE) of photochemical quenching (qp). Different letters above the bars indicate significant differences between treatments (one-way ANOVA followed by Duncan's test:  $p < .05$ ), while same letters above the bars indicate non-significant differences between treatments (one-way ANOVA followed by Duncan's test:  $p > .05$ ). Ozone, time, and species indicate O<sub>3</sub> treatments, different time points, and different cultivars.



30%, and 9% in NF40 and by 27%, 41%, and 46% in NF80 at 60, 90, and 120 DAF, respectively (Figure 2d). The stomatal conductance ( $g_s$ ) decreased by 22%, 17%, and 23% in NF40 and by 23%, 33%, and 39% in NF80 at 60, 90, and 120 DAF, respectively (Figure 2e). Large diurnal changes in  $A_{sat}$  and  $g_s$  were also observed between plants subjected to  $O_3$  treatments every 2–3 h from 10:00 to 16:00 in “Schloss Mannheim” (Figure S2).

As with gas exchange, chlorophyll fluorescence was significantly influenced by  $O_3$  treatment only for “Schloss Mannheim” (Figure 2f–h; Table S4). In this cultivar, the efficiency of excitation energy captured by open PSII reaction centers ( $F_v'/F_m'$ ) decreased by 2%, 11%, 6%, and 5% compared to control in plants subjected to NF40 treatment at 30, 60, 90, and 120 DAF, respectively.  $F_v'/F_m'$  was even more severely reduced by NF80 treatment, decreasing by 4%, 29%, 13%, and 18% relative to the control at 30, 60, 90, and 120 DAF, respectively (Figure 2f). Furthermore, compared to the control, the quantum yield of PSII electron transport ( $\Phi_{PSII}$ ) decreased by 2%, 22%, 28%, and 8% in plants subjected to NF40 treatment and by 14%, 20%, 35%, and 44% in plants subjected to NF80 treatment at 30, 60, 90, and 120 DAF, respectively (Figure 2g). Similar trends were observed for photochemical quenching (qP) (Figure 2h). Thus, both prolonged exposure time and increased exposure concentration had increasingly damaging effects on the pigment contents and physiological characteristics of “Schloss Mannheim,” which was more sensitive to the effects of  $O_3$  than “Iceberg,” “Lüye,” and “Spectra.”

### 3.3 | The $O_3$ -sensitive cultivar exhibits decreased stomatal aperture size when exposed to $O_3$

Stomatal aperture and leaf ultrastructure differed significantly among cultivars under NF80 treatment, as revealed by SEM imaging (Figures 3a and S3–S6). In “Schloss Mannheim,” the stomatal width decreased from  $14.78 \pm .37$  to  $12.08 \pm .28$   $\mu\text{m}$ , stomatal area decreased from  $360.34 \pm 12.71$  to  $283.67 \pm 7.88$   $\mu\text{m}^2$ , and stomatal aperture decreased from  $6.91 \pm .32$  to  $3.44 \pm .26$   $\mu\text{m}$  when plants were exposed to NF80 versus control plants ( $p < .05$ ,  $n = 80$ ) (Figure 3b).  $O_3$  also altered the appearance of epidermal wax in “Schloss Mannheim” (Figures S3–S6). In “Iceberg,” “Lüye,” and “Spectra,” the stomatal shape and epidermis appeared similar between control and treated plants (Figures S3–S6), and there were no significant differences in stomatal length, width, area, or aperture ( $p > .05$ ,  $n = 80$ ) (Figure 3b) or in upper epidermal morphology (Figures S3–S6). Collectively, these data indicate that rose cultivars can be classified as sensitive or tolerant to  $O_3$  according to their somewhat different stomatal behaviors.

### 3.4 | $O_3$ triggers different gene expression patterns in sensitive and resistant rose cultivars

We investigated the effects of  $O_3$  at the molecular level by analyzing the expression profiles of various TF genes and their potential related

genes in stress-related signaling pathways (Figure 4a). We then performed Kyoto Encyclopedia of genes and genomes (KEGG) analysis to identify enriched pathways contributed by the 315 core  $O_3$  responsive DEGs under different treatments at 60 DAF, the 278 core  $O_3$  responsive DEGs under different treatments at 120 DAF. Phenylpropanoid biosynthesis, starch, and sucrose metabolism were the most significantly enriched KEGG pathway followed by MAPK signaling pathway—plant, sesquiterpenoid, and triterpenoid biosynthesis, indicating that phenylpropanoid, starch, and sucrose play key roles under NF and NF80 treatments at 60 DAF in rose (Figure 4b). Similarly, carbon metabolism, phenylpropanoid biosynthesis, and plant hormone signal transduction play key roles under NF and NF80 treatments at 120 DAF in rose (Figure S7).

WGCNA analysis was used to analyze the differentially expressed key genes and TFs under different  $O_3$  concentrations. A total of 40,480 non-redundant DEGs were clustered into 23 main branches, each representing a module (using different color marks) (Figure 4c). Through correlation analysis between co-expression modules and samples of different treatments, it is indicated that red and yellow modules are positively correlated with  $O_3$  response (correlation coefficient  $>.5$ ,  $0 < p < .05$ ), indicating that genes in red and yellow modules play an important role in the response of  $O_3$  response (Figure 4d). Key genes in the red and yellow modules include HSF TF, MYB TF, WRKY TF, cytochrome P450, glucosyltransferase, protein phosphatase 2C, and abscisic acid receptor PYL (Table S5).

Then, the expression level of key genes in red and yellow modules, MYB TFs involved in abiotic stress (*RhMYB62* and *RhMYB108*), and genes involved in ABA signaling pathway (*NCED1*, *OST1*, and *BG1*) were detected and verified by qRT-PCR (Figures 5, S8, and S9). Significant increases in transcript levels relative to the control were observed for TF genes *HSF*, *WRKY*, and *MYB* genes in “Schloss Mannheim” at all time points following exposure to  $O_3$  (NF40 or NF80), and these increases were greater with longer exposure time and higher  $O_3$  concentration. No increases were detected in the other cultivars (Figure 5). In “Schloss Mannheim,” the expression levels of the ABA biosynthesis and signaling-related genes *PP2C*, *PYR1*, *PYL4*, *UGT85A*, and *UGT72E* increased following exposure to either NF40 or NF80 at 30, 60, and 90 DAF (to approximately twofold and threefold higher). The expression levels of these genes did not increase in the other cultivars after  $O_3$  exposure (Figures 5, S8, and S9).

Correlations between the physiological parameters and gene expressions are summarized in Tables S6 and S7. Among these parameters, the physiological parameters had similar patterns of correlation with each other, while the TF genes had similar patterns of correlation with ABA biosynthesis and signaling-related genes. Principal component analysis (PCA) of the interrelationships between physiological parameters and gene expressions revealed that the first three PCA components explained 79.41% of the variance in expression in response to  $O_3$  (Figure 6). The first axis explained 48.12% of the variance and was positively correlated with the expression of the key TF genes *HSF*, *WRKY*, and *MYB* genes and the ABA biosynthesis and signaling-related genes, *PP2C*, *PYR1*, *PYL4*, *UGT85A*, and *UGT72E*, indicating that the variation in the transcript levels of these genes

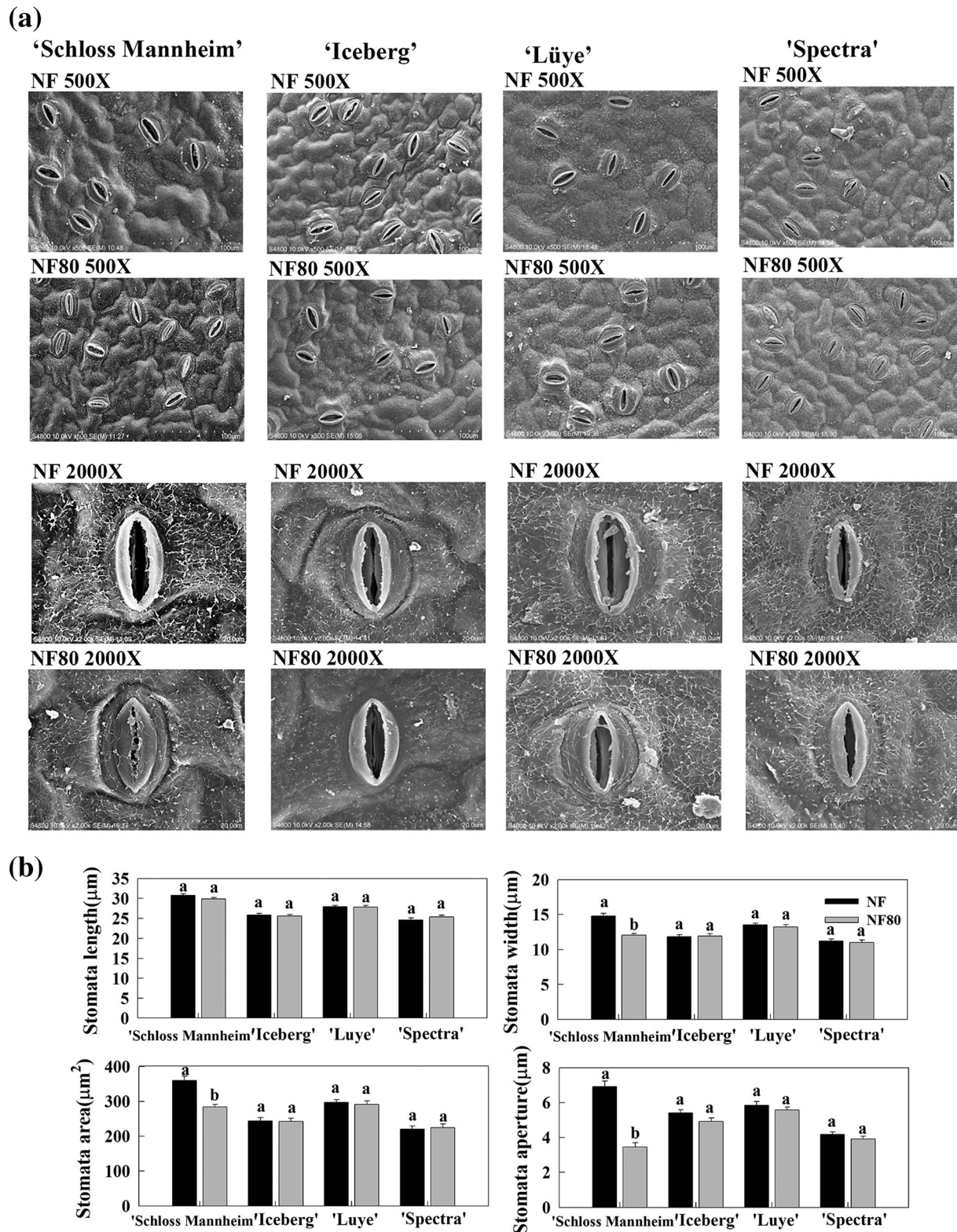


**FIGURE 3** Effects of  $\text{O}_3$  on leaf stomata of rose cultivars "Schloss Mannheim," "Iceberg," "Lüye," and "Spectra" at 120 DAF. (a) Scanning electron microscopy images of the abaxial (lower) and adaxial (upper) leaf surfaces at 120 DAF under various magnifications. (b) Mean value (mean  $\pm$  SE,  $n = 50$ ) of stomatal length, width, area, and aperture changes under different  $\text{O}_3$  treatments. Bar, 100 and 20  $\mu\text{m}$  in SEM images obtained at 500X and 2,000X magnification. Different letters above the bars indicate significant differences between treatments (one-way ANOVA followed by Duncan's test:  $p < .05$ ), while same letters above the bars indicate non-significant differences between treatments (one-way ANOVA followed by Duncan's test:  $p > .05$ ).

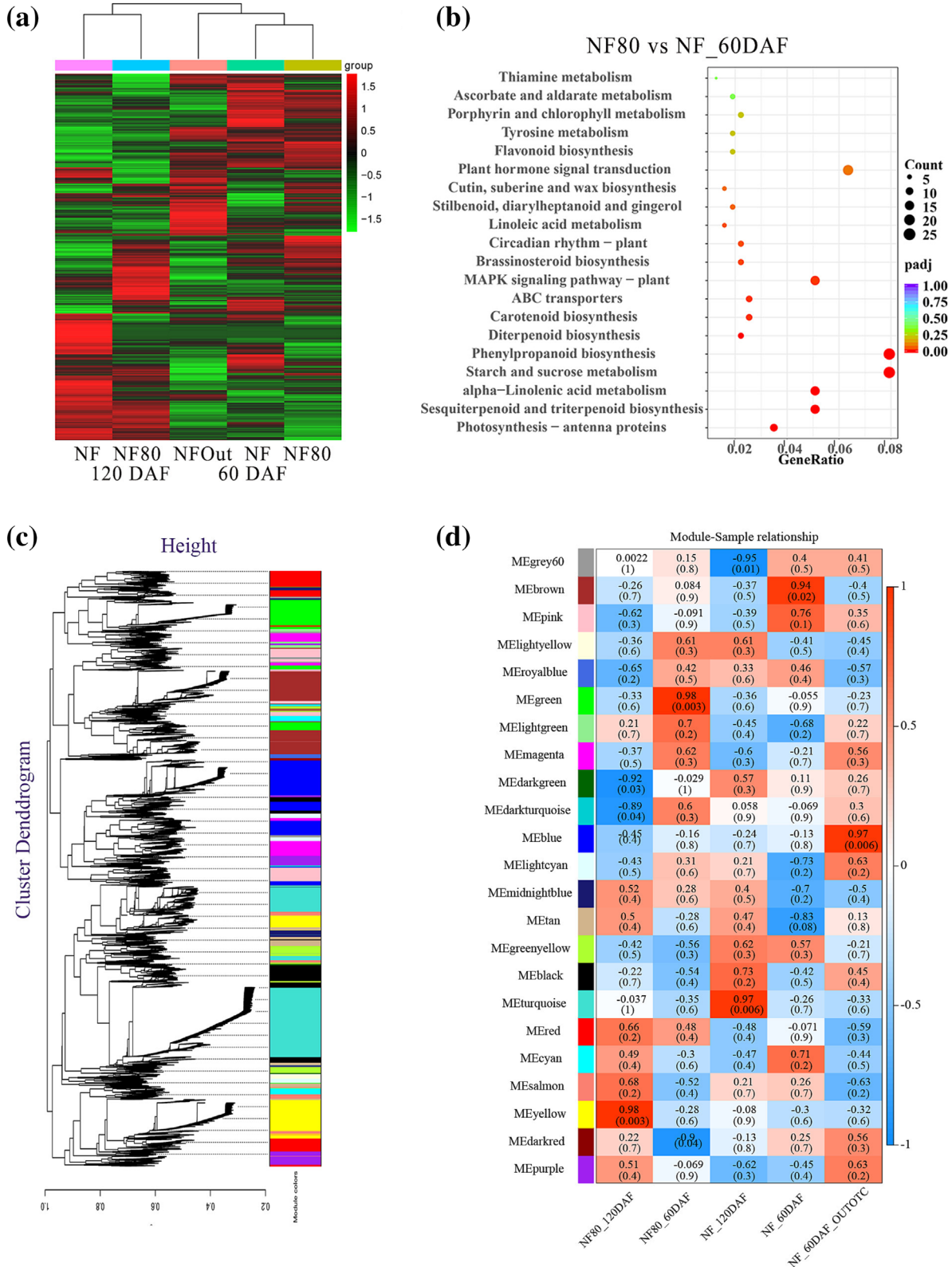


**FIGURE 4** RNA-seq and weighted gene coexpression network analysis (WGCNA) was conducted using leaves samples from O<sub>3</sub> stress and control treatments collected at 60 and 120DAF in O<sub>3</sub>-sensitive cultivar “Schloss Mannheim.” (a) Expression profiles of the ozone responsive DEGs based on fragments per kilobase of transcript per million fragments mapped (FPKM) values. (b) Kyoto Encyclopedia of Genes and Genomes (KEGG) enrichment analyses of ozone responsive DEGs. (c) Hierarchical clustering showing 23 modules of coexpressed genes. (d) WGCNA analysis for differentially expressed genes. Corresponding *p* values of module-sample correlations are indicated in parenthesis. The panel on the left side shows the 23 modules. The color scale on the right side shows module-trait correlation from -1 (blue) to 1 (red).

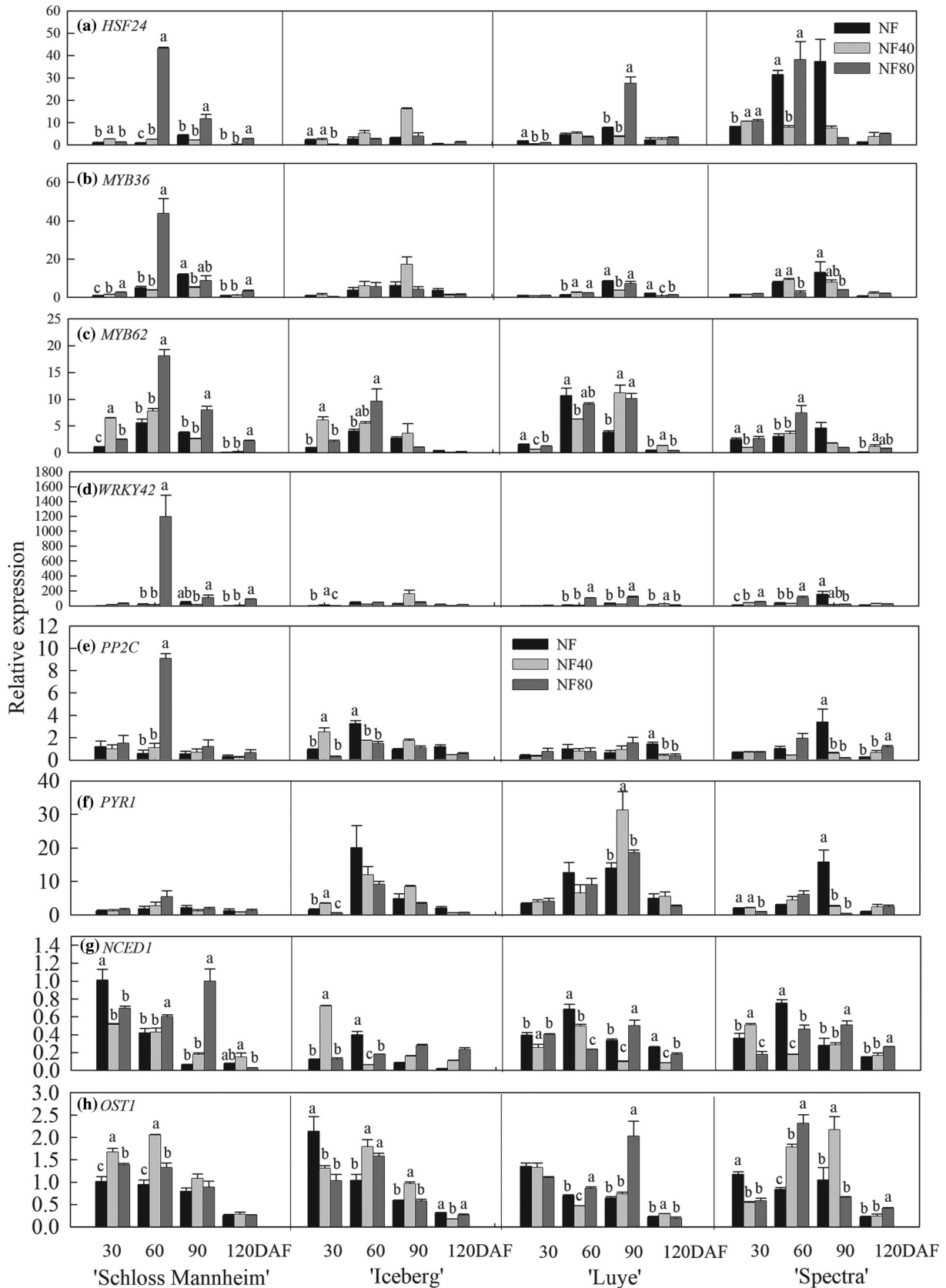
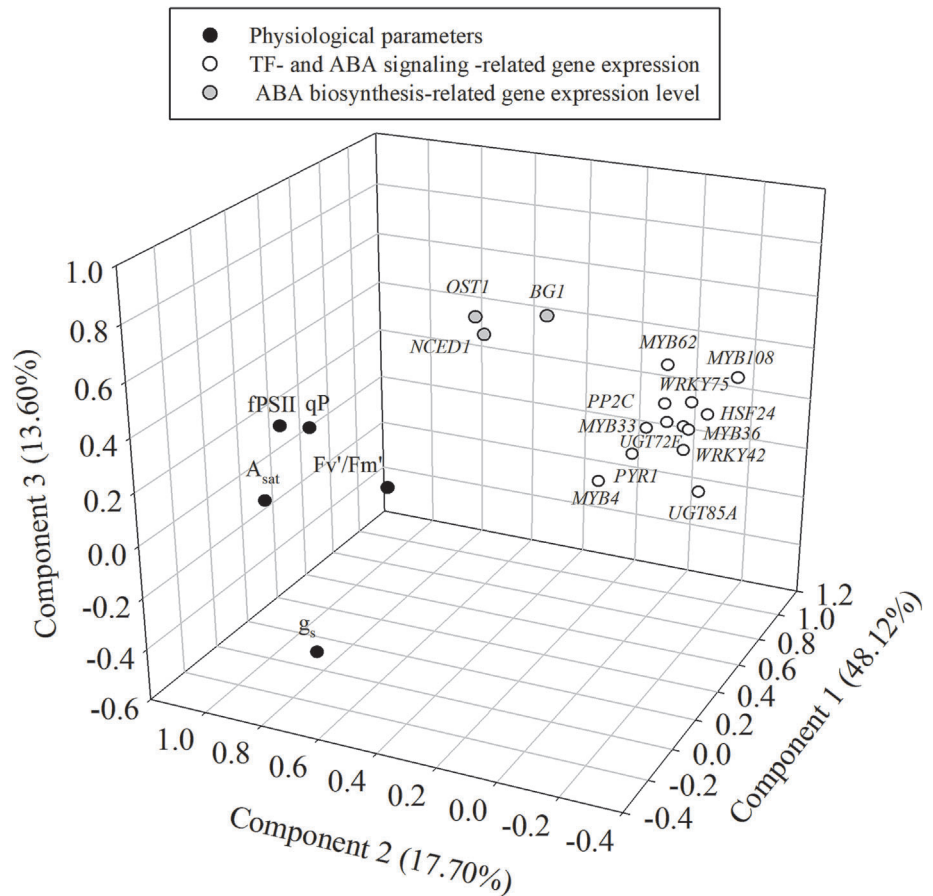


**FIGURE 5** Expression analysis of TF genes, ABA biosynthesis, and signaling-related genes in response to O<sub>3</sub> treatment (NF, NF40, or NF80) in rose cultivars “Schloss Mannheim,” “Iceberg,” “Luye,” and “Spectra” at 30, 60, 90, and 120 DAF. Different letters above the bars indicate significant differences between treatments at p < .05.

**FIGURE 6** Principal component analysis biplot of the physiological parameters and gene expressions levels in response to  $O_3$  in the leaves of  $O_3$  sensitive cultivar. Black dots indicate physiological parameters; white dots indicate TF-related and ABA signaling-related gene expression levels; gray dots indicate ABA biosynthesis-related gene expression levels.



directly influenced physiological responses to  $O_3$  stress via ABA signal transduction. The second axis explained 17.70% of the variance and was positively correlated with change of  $A_{\text{sat}}$ ,  $g_s$ ,  $F_v'/F_m'$ ,  $\Phi\text{PSII}$ ,  $qP$ , indicating that the variation in the physiological parameters directly influenced responses to  $O_3$  stress. The third axis explained 13.60% of the variance and was positively correlated variance and was positively correlated with key genes  $NCED1$ ,  $OST1$ , and  $BG1$ , indicating that these genes directly influenced physiological responses of rose to  $O_3$  stress via ABA biosynthesis. Under elevated  $O_3$ , the expression levels of TF genes  $HSF$ ,  $WRKY$ , and  $MYB$  genes were closely related to those of  $NCED1$ ,  $OST1$ ,  $BG1$ ,  $UGT72E$ ,  $PP2C$ ,  $PYR1$ ,  $PYL4$ , and  $UGT85A$ .

## 4 | DISCUSSION

### 4.1 | Biochemical responses of rose plants to $O_3$ stress

Plant responses to  $O_3$  stress are complex and are mediated by multiple biochemical mechanisms. Even varieties or accessions within the same species may display highly varied molecular and physiological responses to  $O_3$ , as demonstrated in this study. Plant responses to  $O_3$  involve massive changes in gene expression, beginning even before tissue damage is detected. The signaling pathways induced by  $O_3$  are directly related to apoplastic ROS signaling. In the model plant

*Arabidopsis*, phytohormonal signals determine the outcome of  $O_3$  responses at the cellular level, and ROS resulting from  $O_3$  degradation can induce programmed cell death (Kangasjarvi et al., 2005; Xu et al., 2015). A recent study found that *Arabidopsis* accessions Sha and Cvi-0 had accession-specific transcriptional responses to  $O_3$  (Morales et al., 2021). This further demonstrates the notion that the  $O_3$  sensitivity of a plant is strongly influenced by genetic diversity.

Plants use TFs to regulate gene expression. TFs have been shown to regulate the  $O_3$  stress response in plants by activating stress response genes. TFs (Marchica et al., 2019; Xu et al., 2015; Zhang et al., 2019, 2022) regulate at least some aspects of the  $O_3$  response. ABA biosynthesis and signaling-related genes, including  $NCED$ ,  $OST1$  (encoding a SNF1-related protein kinase),  $PP2C$  (encoding a type 2C protein phosphatase),  $O_3$  stress-regulated genes, and antioxidant response genes (e.g.,  $APX$ ,  $GST$ , and  $GPX$ ), regulate stomatal movement via ABA and act upstream of ROS production (McAdam et al., 2017; Mustilli et al., 2002). However, several TFs that have yet to be identified are likely also involved in the  $O_3$  response. Here, we used WGCNA analysis of transcriptome datasets from  $O_3$  stress and control conditions and revealed novel genes and the molecular pathways underlying rose response to  $O_3$  stress. The plant hormone abscisic acid (ABA) acts as a developmental signal and as an integrator of  $O_3$  stress. Key players in ABA signal transduction include the type 2C protein phosphatases (PP2Cs), which act by negatively regulating ABA responses (Ma et al., 2009). Consistent with this, in the sensitive

cultivar, stomatal closure occurred concomitantly with the increase of *NCED1*, *PP2Cs*, and *PYR/PYL* receptors expression level, which induced ABA accumulation in the leaves under ozone stress. Our result also provides further evidence of the role of ABA acting as a developmental signal and as an integrator of  $O_3$  stress. Moreover, some studies suggest that WRKYs could play a pivotal role in the signaling mechanisms during the responses of plants to  $O_3$  (Marchica et al., 2019; Zhang et al., 2022). *RcWRKY42* and *RcWRKY75* were highly expressed in response to  $O_3$  stress. *RcHSF24*, *RcMYB4*, *RcMYB36*, *RcMYB33*, *MYB62*, and *MYB108* were also highly expressed in response to  $O_3$  stress. Hence, we evaluated the expression of *HSF*, *WRKY*, and *MYB* genes, which correlated with the transcription of ABA biosynthesis and signaling-related genes including *NCED1*, *PP2Cs*, *PYR/PYL*, and *UGTs* as part of an  $O_3$  stress response.

We characterized the physiological and molecular responses of leaves from different rose cultivars to  $O_3$  stress. For the  $O_3$ -sensitive rose variety “Schloss Mannheim,” we propose that  $O_3$  functions as a signaling molecule that triggers the expression of core TF genes. These TFs then act either alone or with other proteins to form an activation complex, which correlate with the transcription of key ABA biosynthesis and signaling-related genes. This leads to the accumulation of ABA, which promotes stomatal closure, a reduction in pigment contents, and the depression of the net photosynthetic rate and stomatal conductance, leading to visible symptoms and stunted growth. For the  $O_3$ -resistant rose cultivars “Iceberg,” “Lüye,” and “Spectra,” these trends were not observed (Figure 7).

## 4.2 | Sensitivity of rose cultivars to $O_3$ stress

The varieties and accession of same species show varied response. Purple-leafed Pakchoi cultivars with higher anthocyanin contents

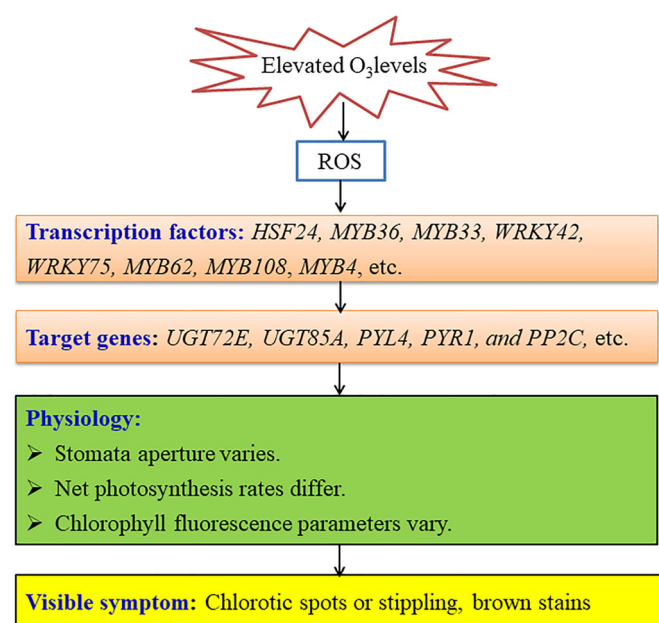


**FIGURE 7** Model depicting plant responses to  $O_3$  stress.

were more tolerant than green-leafed cultivars as indicated by lower relative enhancement in malondialdehyde content and lower relative losses in  $P_N$ ,  $g_s$ ,  $F_v/F_m$ , and  $Y_{II}$  (Zhang et al., 2017). The order of  $O_3$  sensitivity in five poplar clones was clone DQ, 546, WQ156, 84 K, and 107 (Shang et al., 2020). The growth and biochemistry of castor cultivar Shivam are highly correlating with treatments suggested its highest sensitivity for ozone pollution while negative PCA score of cultivar Nidhi-999 suggested reduced responsiveness for ozone pollution (Rathore & Chaudhary, 2019). Consistent with these results, among the four rose cultivars tested in this study, “Schloss Mannheim” was the most  $O_3$  sensitive, whereas “Iceberg,” “Lüye,” and “Spectra” were much more  $O_3$  tolerant. These cultivars are more likely to survive and tolerate high  $O_3$  levels. Visible foliar injury is not consistent with AOT40, as AOT40 does not keep into account ozone stomatal flux, which apparently differs in the sensitive and resistant cultivars. In general, in severely  $O_3$ -polluted areas such as several cities in China, plants with highly efficient biochemical processes and robust photosynthetic performance are recommended for landscaping and other horticultural uses.

Numerous studies have shown that  $O_3$  can induce visible injury to leaves and that visible foliar injury may indicate plant sensitivity to  $O_3$  (Li et al., 2015; Rathore & Chaudhary, 2019; Shang et al., 2020; Yang et al., 2016; Zhang & Sonnewald, 2017).  $O_3$  primarily enters plants through the stomata of leaves, and leaf  $g_s$  has been used to calculate the  $O_3$  uptake rate in plants (Paoletti, 2006). Some studies have shown that leaf  $g_s$  is another indicator of  $O_3$  sensitivity in plants, with higher  $g_s$  indicating higher  $O_3$  flux into the plant. In this study, among the cultivars tested, only the  $O_3$ -sensitive cultivar “Schloss Mannheim” showed a significant reduction in average stomatal aperture size when exposed to  $O_3$ . For this cultivar, stomatal closure likely inhibits photosynthetic efficiency, leading to subsequent leaf pathologies. It is worth noting that Stomatal conductance is decreased by 39% but stomatal aperture is halved by NF80 treatment at 120 DAF. The difference is ascribed to the sampling area of leaf for gas-exchange measurements is  $6\text{ cm}^2$  and for histological observations is  $.4\text{ cm}^2$ , which only included the chlorotic spots. Photosynthetic parameters associated with the dark reactions of photosynthesis were more efficient in “Iceberg,” “Lüye,” and “Spectra,” likely due to the superior antioxidant capacities of these plants. This putative physiological mechanism is consistent with morphological observations of stomatal width, area, and aperture size, which were essentially unchanged for the  $O_3$ -tolerant cultivars. Thus, based on stomatal behavior, the rose cultivars examined in this study could be identified as either sensitive or tolerant to  $O_3$ .

In conclusion, we determined that rose cultivar “Schloss Mannheim” is sensitive to  $O_3$  based on its visible foliar injury, reduced gas-exchange capacity, and suppressed chlorophyll fluorescence parameters when exposed to high  $O_3$  levels. Moreover, this cultivar showed significant reductions in stomatal width, area, and aperture size upon exposure to  $O_3$ .  $O_3$  functions as a signaling molecule that triggers the expression of core TF genes (*HSF*, *WRKY*, and *MYB* genes), which correlated with key ABA biosynthesis and signaling-related genes (*NCED1*, *PP2Cs*, *PYR/PYL*, and *UGTs*) whose increased



expression leads to ABA accumulation, stomatal closure, reduced pigment contents, depression of the photosynthetic rate and stomatal conductance, and ultimately visible damage and stunted growth. The results of this study reveal some of the integrated physiological and molecular mechanisms that may confer O<sub>3</sub> sensitivity or tolerance to rose cultivars. This information may improve rose management in urban settings.

## AUTHOR CONTRIBUTIONS

Wanmei Jin and Zhaozhong Feng conceived and designed the experiments; Hua Wang, Maofu Li, Yuan Yang, Pei Sun, Shuting Zhou, and Yanhui Kang performed the research; Yansen Xu and Xiangyang Yuan managed the rose cultivars and open-top chambers; Hua Wang, Maofu Li, and Wanmei Jin carried out the data analyses; Hua Wang, Zhaozhong Feng, and Wanmei Jin wrote the manuscript.

## ACKNOWLEDGMENTS

The research was supported by the National Natural Science Foundation for Young Scholars of China (31600418) and the Science and Technology Innovation Ability Construction Projects of Beijing Academy of Agriculture and Forestry Science (KJCX20230110 and KJCX20210415).

## CONFLICT OF INTEREST STATEMENT

The authors have no conflict of interest to declare.

## DATA AVAILABILITY STATEMENT

All data supporting the findings of this study are available within the paper and within its supplementary data published online.

## ORCID

Maofu Li  <https://orcid.org/0000-0003-3215-0049>

Wanmei Jin  <https://orcid.org/0000-0002-2356-7806>

## REFERENCES

- Ainsworth, E. A. (2017). Understanding and improving global crop response to ozone pollution. *The Plant Journal*, 90, 886–897. <https://doi.org/10.1111/tpj.13298>
- Ashrafuzzaman, M., Haque, Z., Ali, B., Mathew, B., Yu, P., Hochholdinger, F., de Abreu Neto, J. B., McGillen, M. R., Ensikat, H. J., & Manning, W. J. (2018). Ethylenediurea (EDU) mitigates the negative effects of ozone in rice: Insights into its mode of action. *Plant, Cell & Environment*, 41, 2882–2898. <https://doi.org/10.1111/pce.13423>
- Beijing Gardening and Greening Bureau. (2017). *Collection of Beijing urban gardening and afforestation survey, monograph*. Beijing Publishing House.
- Carvalho, D. R. A., Vasconcelos, M. W., Lee, S., Koning-Boucoiran, C. F. S., Vreugdenhil, D., Krens, F. A., Heuvelink, E., & Carvalho, S. M. P. (2016). Gene expression and physiological responses associated to stomatal functioning in *Rosa × hybrida* grown at high relative air humidity. *Plant Science*, 253, 154–163. <https://doi.org/10.1016/j.plantsci.2016.09.018>
- Chappelka, A. H., & Samuelson, L. J. (1998). Ambient ozone effects on forest trees of the eastern United States: A review. *New Phytologist*, 139, 91–108. <https://doi.org/10.1046/j.1469-8137.1998.00166.x>
- Cheng, B., Wan, H., Han, Y., Yu, C., Luo, L., Pan, H., & Zhang, Q. (2021). Identification and QTL analysis of flavonoids and carotenoids in tetraploid roses based on an ultra-high-density genetic map. *Frontiers in Plant Science*, 12, 1071.
- Cotrozzi, L. (2021). The effects of tropospheric ozone on oaks: A global meta-analysis. *Science of the Total Environment*, 756, 143795. <https://doi.org/10.1016/j.scitotenv.2020.143795>
- Engela, M. R. G. S., Furlan, C. M., Esposito, M. P., Fernandes, F. F., Carrari, E., Domingos, M., Paoletti, E., & Hoshika, Y. (2021). Metabolic and physiological alterations indicate that the tropical broadleaf tree *Eugenia uniflora* L. is sensitive to ozone. *Science of the Total Environment*, 769, 145080. <https://doi.org/10.1016/j.scitotenv.2021.145080>
- Eugster, C. H., & Märki-Fischer, E. (1991). The chemistry of rose pigments. *Angewandte Chemie International Edition in English*, 30, 654–672. <https://doi.org/10.1002/anie.199106541>
- Feng, Z., de Marco, A., Anav, A., Gualtieri, M., Sicard, P., Tian, H., Fornasier, F., Tao, F., Guo, A., & Paoletti, E. (2019). Economic losses due to ozone impacts on human health, forest productivity and crop yield across China. *Environment International*, 131, 104966. <https://doi.org/10.1016/j.envint.2019.104966>
- Feng, Z. Z., Kobayashi, K., & Ainsworth, E. A. (2008). Impact of elevated ozone concentration on growth, physiology, and yield of wheat (*Triticum aestivum* L.): A meta-analysis. *Global Change Biology*, 14, 2696–2708. <https://doi.org/10.1111/j.1365-2486.2008.01673.x>
- Feng, Z., Sun, J., Wan, W., Hu, E., & Calatayud, V. (2014). Evidence of widespread ozone-induced visible injury on plants in Beijing, China. *Environmental Pollution*, 193, 296–301. <https://doi.org/10.1016/j.envpol.2014.06.004>
- Feng, Z., Xu, Y., Kobayashi, K., Dai, L., Zhang, T., Agathokleous, E., Calatayud, V., Paoletti, E., Mukherjee, A., & Agrawal, M. (2022). Ozone pollution threatens the production of major staple crops in East Asia. *Nature Food*, 3, 47–56. <https://doi.org/10.1038/s43016-021-00422-6>
- Han, Y. J., Gharibeshghi, A., Mewis, I., Förster, N., Beck, W., & Ulrichs, C. (2021). Effect of different durations of moderate ozone exposure on secondary metabolites of *Brassica campestris* L. ssp. *chinensis*. *The Journal of Horticultural Science and Biotechnology*, 96, 110–120. <https://doi.org/10.1080/14620316.2020.1793692>
- Hasan, M. M., Rahman, M. A., Skalicky, M., Alabdallah, N. M., Waseem, M., Jahan, M. S., Ahammed, G. J., El-Mogy, M. M., El-Yazied, A. A., Ibrahim, M. F. M., & Fang, X.-W. (2021). Ozone induced stomatal regulations, MAPK and phytohormone signaling in plants. *International Journal of Molecular Sciences*, 22, 6304. <https://doi.org/10.3390/ijms22126304>
- Holder, A. J., & Hayes, F. (2022). Substantial yield reduction in sweet potato due to tropospheric ozone, the dose-response function. *Environmental Pollution*, 304, 119209. <https://doi.org/10.1016/j.envpol.2022.119209>
- Iyer, N. J., Tang, Y., & Mahalingam, R. (2013). Physiological, biochemical and molecular responses to a combination of drought and ozone in *Medicago truncatula*. *Plant, Cell & Environment*, 36, 706–720. <https://doi.org/10.1111/pce.12008>
- Jin, W., Wang, H., Li, M., Wang, J., Yang, Y., Zhang, X., Yan, G., Zhang, H., Liu, J., & Zhang, K. (2016). The R2R3 MYB transcription factor *Pav-MYB10.1* involves in anthocyanin biosynthesis and determines fruit skin colour in sweet cherry (*Prunus avium* L.). *Plant Biotechnology Journal*, 14, 2120–2133. <https://doi.org/10.1111/pbi.12568>
- Kakani, V. G., Reddy, K. R., Zhao, D., & Mohammed, A. R. (2003). Effects of ultraviolet-B radiation on cotton (*Gossypium hirsutum* L.) morphology and anatomy. *Annals of Botany*, 91, 817–826. <https://doi.org/10.1093/aob/mcg086>
- Kangasjarvi, J., Jaspers, P., & Kollist, H. (2005). Signalling and cell death in ozone-exposed plants. *Plant, Cell & Environment*, 28, 1021–1036. <https://doi.org/10.1111/j.1365-3040.2005.01325.x>

- Kontunen-Soppela, S., Riikonen, J., Ruhanen, H., Brosché, M., Somervuo, P., Peltonen, P., Kangasjärvi, J., Auvinen, P., Paulin, L., Keinänen, M., Oksanen, E., & Vapaavuori, E. (2010). Differential gene expression in senescing leaves of two silver birch genotypes in response to elevated CO<sub>2</sub> and tropospheric ozone. *Plant, Cell & Environment*, 33, 1016–1028. <https://doi.org/10.1111/j.1365-3040.2010.02123.x>
- Leisner, C. P., & Ainsworth, E. A. (2012). Quantifying the effects of ozone on plant reproductive growth and development. *Global Change Biology*, 18, 606–616. <https://doi.org/10.1111/j.1365-2486.2011.02535.x>
- Leisner, C. P., Ming, R., & Ainsworth, E. A. (2014). Distinct transcriptional profiles of ozone stress in soybean (*Glycine max*) flowers and pods. *BMC Plant Biology*, 14, 335.
- Leus, L., van Laere, K., de Riek, J., & van Huylenbroeck, J. (2018). *Rose. Ornamental crops* (pp. 719–767). Springer.
- Li, L., Manning, W. J., Tong, L., & Wang, X. (2015). Chronic drought stress reduced but not protected Shantung maple (*Acer truncatum* Bunge) from adverse effects of ozone (O<sub>3</sub>) on growth and physiology in the suburb of Beijing, China. *Environmental Pollution*, 201, 34–41. <https://doi.org/10.1016/j.envpol.2015.02.023>
- Lichtenthaler, H. K. (1987). Chlorophyll fluorescence signatures of leaves during the autumnal chlorophyll breakdown. *Journal of Plant Physiology*, 131, 101–110. [https://doi.org/10.1016/S0176-1617\(87\)80271-7](https://doi.org/10.1016/S0176-1617(87)80271-7)
- Livak, K. J., & Schmittgen, T. D. (2001). Analysis of relative gene expression data using real-time quantitative PCR and the 2<sup>-ΔΔCT</sup> method. *Methods*, 25, 402–408. <https://doi.org/10.1006/meth.2001.1262>
- Ma, Y., Szostkiewicz, I., Korte, A., Moes, D., Yang, Y., Christmann, A., & Grill, E. (2009). Regulators of PP2C phosphatase activity function as abscisic acid sensors. *Science*, 324, 1064–1068. <https://doi.org/10.1126/science.1172408>
- Magnard, J.-L., Rocca, A., Caissard, J.-C., Vergne, P., Sun, P., Hecquet, R., Dubois, A., Hibrand-Saint Oyant, L., Jullien, F., Nicolè, F., Raymond, O., Huguet, S., Baltenweck, R., Meyer, S., Claudel, P., Jeauffre, J., Rohmer, M., Foucher, F., Huguency, P., ... Baudino, S. (2015). Biosynthesis of monoterpene scent compounds in roses. *Science*, 349, 81–83. <https://doi.org/10.1126/science.aab0696>
- Marchica, A., Lorenzini, G., Papini, R., Bernardi, R., Nali, C., & Pellegrini, E. (2019). Signalling molecules responsive to ozone-induced oxidative stress in *Salvia officinalis*. *Science of the Total Environment*, 657, 568–576. <https://doi.org/10.1016/j.scitotenv.2018.11.472>
- McAdam, E. L., Brodrick, T. J., & McAdam, S. A. M. (2017). Does ozone increase ABA levels by non-enzymatic synthesis causing stomata to close? *Plant, Cell & Environment*, 40, 741–747. <https://doi.org/10.1111/pce.12893>
- Morales, L. O., Shapiguzov, A., Safronov, O., Leppälä, J., Vaahtera, L., Yarmolinsky, D., Kollist, H., & Brosché, M. (2021). Ozone responses in *Arabidopsis*: Beyond stomatal conductance. *Plant Physiology*, 186, 180–192. <https://doi.org/10.1093/plphys/kiab097>
- Mustilli, A.-C., Merlot, S., Vavasseur, A., Fenzi, F., & Giraudat, J. (2002). Arabidopsis OST1 protein kinase mediates the regulation of stomatal aperture by abscisic acid and acts upstream of reactive oxygen species production. *The Plant Cell*, 14, 3089–3099. <https://doi.org/10.1105/tpc.007906>
- Nadpal, J. D., Lesjak, M. M., Šibul, F. S., Anačkov, G. T., Četojević-Simin, D. D., Mimica-Dukić, N. M., & Beara, I. N. (2016). Comparative study of biological activities and phytochemical composition of two rose hips and their preserves: *Rosa canina* L. and *Rosa arvensis* Huds. *Food Chemistry*, 192, 907–914. <https://doi.org/10.1016/j.foodchem.2015.07.089>
- Nowak, D. J., & Dwyer, J. F. (2007). Understanding the benefits and costs of urban forest ecosystems. In J. E. Kuser (Ed.), *Urban and community forestry in the northeast* (pp. 25–46). Springer Science and Business Media. [https://doi.org/10.1007/978-1-4020-4289-8\\_2](https://doi.org/10.1007/978-1-4020-4289-8_2)
- Paoletti, E. (2006). Impact of ozone on Mediterranean forests: A review. *Environmental Pollution*, 144, 463–474. <https://doi.org/10.1016/j.envpol.2005.12.051>
- Peng, J., Xu, Y., Shang, B., Qu, L., & Feng, Z. (2020). Impact of ozone pollution on nitrogen fertilization management during maize (*Zea mays* L.) production. *Environmental Pollution*, 266, 115158. <https://doi.org/10.1016/j.envpol.2020.115158>
- Rathore, D., & Chaudhary, I. J. (2019). Ozone risk assessment of castor (*Ricinus communis* L.) cultivars using open top chamber and ethylene-dioxide (EDU). *Environmental Pollution*, 244, 257–269. <https://doi.org/10.1016/j.envpol.2018.10.036>
- Raymond, O., Guzy, J., Just, J., Badouin, H., Verdenaud, M., Lemaingué, A., Vergne, P., Moja, S., Choisine, N., Pont, C., Carrère, S., Caissard, J.-C., Couloux, A., Cottret, L., Aury, J.-M., Szécsi, J., Latrasse, D., Madoui, M.-A., François, L., ... Bendahmane, M. (2018). The *Rosa* genome provides new insights into the domestication of modern roses. *Nature Genetics*, 50, 772–777. <https://doi.org/10.1038/s41588-018-0110-3>
- Shang, B., Feng, Z., Gao, F., & Calatayud, V. (2020). The ozone sensitivity of five poplar clones is not related to stomatal conductance, constitutive antioxidant levels and morphology of leaves. *Science of the Total Environment*, 699, 134402. <https://doi.org/10.1016/j.scitotenv.2019.134402>
- Smulders, M. J. M., Arens, P., Bourke, P. M., Debener, T., Linde, M., Riek, J. D., Leus, L., Ruttink, T., Baudino, S., Hibrant Saint-Oyant, L., Clotault, J., & Foucher, F. (2019). In the name of the rose: A roadmap for rose research in the genome era. *Horticulture Research*, 6, 65. <https://doi.org/10.1038/s41438-019-0156-0>
- Wang, Q., Li, Z., Li, X., Ping, Q., Yuan, X., Agathokleous, E., & Feng, Z. (2021). Interactive effects of ozone exposure and nitrogen addition on the rhizosphere bacterial community of poplar saplings. *Science of the Total Environment*, 754, 142134. <https://doi.org/10.1016/j.scitotenv.2020.142134>
- Wang, T., Xue, L., Feng, Z., Dai, J., Zhang, Y., & Tan, Y. (2022). Ground-level ozone pollution in China: A synthesis of recent findings on influencing factors and impacts. *Environmental Research Letters*, 17, 063003. <https://doi.org/10.1088/1748-9326/ac69fe>
- Wang, H., Yang, Y., Li, M., Liu, J., & Jin, W. (2017). Residents' preferences for roses, features of rose plantings and the relations between them in built-up areas of Beijing, China. *Urban Forestry & Urban Greening*, 27, 1–8. <https://doi.org/10.1016/j.ufug.2017.06.011>
- Whaley, A., Sheridan, J., Safari, S., Burton, A., Burkey, K., & Schlueter, J. (2015). RNA-seq analysis reveals genetic response and tolerance mechanisms to ozone exposure in soybean. *BMC Genomics*, 16, 1–13.
- Wu, X., Liang, S., & Byrne, D. H. (2019). Heritability of plant architecture in diploid roses (*Rosa* spp.). *HortScience*, 54, 236–239. <https://doi.org/10.12173/HORTSCI13511-18>
- Wu, Y., Wen, J., Xia, Y., Zhang, L., & Du, H. (2022). Evolution and functional diversification of R2R3-MYB transcription factors in plants. *Horticulture Research*, 9, uhac058. <https://doi.org/10.1093/hr/uhac058>
- Xu, Y., Feng, Z., Shang, B., Dai, L., Uddling, J., & Tarvainen, L. (2019). Mesophyll conductance limitation of photosynthesis in poplar under elevated ozone. *Science of the Total Environment*, 657, 136–145. <https://doi.org/10.1016/j.scitotenv.2018.11.466>
- Xu, E., Vaahtera, L., & Brosché, M. (2015). Roles of defense hormones in the regulation of ozone-induced changes in gene expression and cell death. *Molecular Plant*, 8, 1776–1794. <https://doi.org/10.1016/j.molp.2015.08.008>
- Xu, J.-P., Yu, Y.-C., Zhang, T., Ma, Q., & Yang, H.-B. (2021). Effects of ozone water irrigation and spraying on physiological characteristics and gene expression of tomato seedlings. *Horticulture Research*, 8, 180. <https://doi.org/10.1038/s41438-021-00618-8>
- Yang, N., Wang, X., Cotrozzi, L., Chen, Y., & Zheng, F. (2016). Ozone effects on photosynthesis of ornamental species suitable for urban



- green spaces of China. *Urban Forestry & Urban Greening*, 20, 437–447. <https://doi.org/10.1016/j.ufug.2016.10.014>
- Yendrek, C. R., Koester, R. P., & Ainsworth, E. A. (2015). A comparative analysis of transcriptomic, biochemical, and physiological responses to elevated ozone identifies species-specific mechanisms of resilience in legume crops. *Journal of Experimental Botany*, 66, 7101–7112. <https://doi.org/10.1093/jxb/erv404>
- Zhang, J., Gao, F., Jia, H., Hu, J., & Feng, Z. (2019). Molecular response of poplar to single and combined ozone and drought. *Science of the Total Environment*, 655, 1364–1375. <https://doi.org/10.1016/j.scitotenv.2018.11.195>
- Zhang, H., & Sonnewald, U. (2017). Differences and commonalities of plant responses to single and combined stresses. *The Plant Journal*, 90, 839–855. <https://doi.org/10.1111/tbj.13557>
- Zhang, J., Wang, Y., Mao, Z., Liu, W., Ding, L., Zhang, X., Yang, Y., Wu, S., Chen, X., & Wang, Y. (2022). Transcription factor McWRKY71 induced by ozone stress regulates anthocyanin and proanthocyanidin biosynthesis in *Malus crabapple*. *Ecotoxicology and Environmental Safety*, 232, 113274. <https://doi.org/10.1016/j.ecoenv.2022.113274>
- Zhang, L., Xiao, S., Chen, Y. J., Xu, H., Li, Y. G., Zhang, Y. W., & Luan, F. S. (2017). Ozone sensitivity of four Pakchoi cultivars with different leaf

- colors: Physiological and biochemical mechanisms. *Photosynthetica*, 55, 478–490. <https://doi.org/10.1007/s11099-016-0661-4>
- Zouzoulas, D., Koutroubas, S. D., Vassiliou, G., & Vardavakis, E. (2009). Effects of ozone fumigation on cotton (*Gossypium hirsutum* L.) morphology, anatomy, physiology, yield and qualitative characteristics of fibers. *Environmental and Experimental Botany*, 67, 293–303. <https://doi.org/10.1016/j.envexpbot.2009.05.016>

## SUPPORTING INFORMATION

Additional supporting information can be found online in the Supporting Information section at the end of this article.

**How to cite this article:** Wang, H., Li, M., Yang, Y., Sun, P., Zhou, S., Kang, Y., Xu, Y., Yuan, X., Feng, Z., & Jin, W. (2023). Physiological and molecular responses of different rose (*Rosa hybrida* L.) cultivars to elevated ozone levels. *Plant Direct*, 7(7), e513. <https://doi.org/10.1002/pld3.513>